JACC: BASIC TO TRANSLATIONAL SCIENCE VOL. 8, NO. 6, 2023

ORIGINAL RESEARCH - PRECLINICAL

IGF-1 Therapy Improves Muscle Size and Function in Experimental Peripheral Arterial Disease

Gengfu Dong, MS,[a] Chatick Moparthy,[a] Trace Thome, MS,[a] Kyoungrae Kim, PhD,[a] Feng Yue, PhD,[b,d] Terence E. Ryan, PhD[a,c,d]

VISUAL ABSTRACT

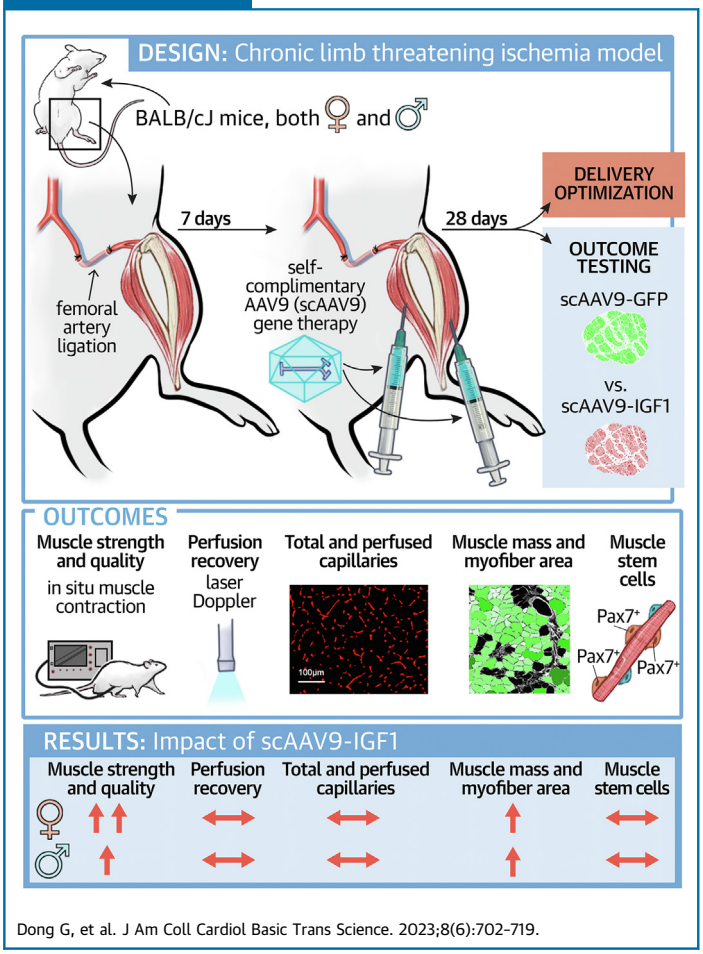

Dong G, et al. J Am Coll Cardiol Basic Trans Science. 2023;8(6):702-719.

HIGHLIGHTS

- **scAAV9 gene therapies can be delivered to, and produce robust transgene expression in, the critically ischemic mouse limb without adverse impact on perfusion recovery or muscle health/function.**
- **Treatment of the ischemic limb with scAAV9-IGF-1 significantly improved muscle size and strength in male and female mice with hindlimb ischemia.**
- **Differences in the efficacy of scAAV9-IGF-1 were observed, with female mice displaying greater improvements in muscle contractile function than male mice.**
- **IGF-1-mediated improvements in muscle function occurred without changes in limb perfusion recovery or capillary density.**

From the [a]Department of Applied Physiology and Kinesiology, University of Florida, Gainesville, Florida, USA; [b]Department of Animal Sciences, University of Florida, Gainesville, Florida, USA; [c]Center for Exercise Science, University of Florida, Gainesville, Florida, USA; and the [d]Myology Institute, University of Florida, Gainesville, Florida, USA.

ISSN 2452-302X https://doi.org/10.1016/j.jacbts.2022.12.006

SUMMARY

Lower-extremity peripheral arterial disease (PAD) has increased in prevalence, yet therapeutic development has remained stagnant. Skeletal muscle health and function has been strongly linked to quality of life and medical outcomes in patients with PAD. Using a rodent model of PAD, this study demonstrates that treatment of the ischemic limb with insulin-like growth factor (IGF)-1 significantly increases muscle size and strength without improving limb hemodynamics. Interestingly, the effect size of IGF1 therapy was larger in female mice than in male mice, highlighting the need to carefully examine sex-dependent effects in experimental PAD therapies.

ABBREVIATIONS AND ACRONYMS

AAV = adeno-associated virus

scAAV9 = self-complimentary adeno-associated virus serotype 9

CLTI = chronic limb-threatening ischemia

CMV = cytomegalovirus

CSA = cross-sectional area

EDL = extensor digitorum longus

FAL = femoral artery ligation

FDB = flexor digitorum brevis

GFP = green fluorescent protein

IGF = insulin-like growth factor

IGFBP3 = insulin-like growth factor–binding protein 3

PAD = peripheral arterial disease

TA = tibialis anterior

Peripheral arterial disease (PAD), caused by atherosclerotic narrowing or occlusion of blood vessels in the lower extremities,[1] affects an estimated 200 million people throughout the world,[2,3] making it the third-leading cause of the cardiovascular death.[3] A small proportion of patients with PAD develop chronic limb-threatening ischemia (CLTI), the condition's most severe manifestation, which is characterized by chronic ischemic rest pain that can occur with or without nonhealing wounds, ulcers, or gangrene.[4] Based on the symptom severity, patients with CLTI have an increased risk of lower-extremity amputation and cardiovascular mortality compared to PAD patients without CLTI.[4] Primary treatments for CLTI include endovascular and revascularization surgeries aimed to improve blood flow to the affected limb.[5,6] Despite advances in surgical techniques, the complexity of CLTI pathobiology and the moderate-to-high risk classification of most CLTI patients contribute to unfavorable failure rates.[7-10] Unfortunately, nonsurgical medical therapy is limited to risk factor-modifying treatments, such as antithrombotic, antihypertensive, lipid-lowering, and glucose-controlling medications. These therapies are effective for reducing cardiovascular events such as myocardial infarction and stroke, but unfortunately they do not significantly improve walking performance or functional ability in patients with PAD. Thus, there is a substantial need to develop new medical therapies that can be effective at improving limb function and outcomes in PAD/CLTI.

Gene- and cell-based regenerative therapies have emerged as leading technologies for the treatment of numerous human diseases. Specifically, adeno-associated viruses (AAVs), nonpathogenic DNA viruses, have been successfully used to treat spinal muscular atrophy and retinal dystrophy in humans, and numerous other AAV-based gene therapies are currently in clinical trials. Several clinical trials have tested gene or cell therapies in PAD/CLTI, although to date none have proven to be effective.[11-14] The lack of success in translating gene- and cell-based therapies to PAD patients with severe claudication or patients with CLTI is multifactorial and undoubtedly involves the heterogeneity of patient characteristics. Furthermore, early-stage preclinical models may not have adequately modeled the CLTI condition. The majority of gene- and cell-based therapies have been applied in mouse and rat models of hindlimb ischemia (femoral artery ligation), but the therapeutic has been most commonly applied either before or immediately after surgery, before the severe ischemic tissue pathology has developed.[15-24] Obviously, the timing of these treatments is not directly relevant to the PAD/CLTI patient, who is generally referred to a specialist after the development of symptoms. Moreover, most studies have used the C57BL6 genetic background, which is known to recover rapidly from hindlimb ischemia, does not develop the CLTI phenotype,[21,22,25-27] and is resistant to acute ischemic injury compared with the BALB/c mouse.[28]

In the present study, we first aimed to optimize the dosing and injection strategy for the delivery of self-complimentary adeno-associated virus serotype 9

The authors attest they are in compliance with human studies committees and animal welfare regulations of the authors' institutions and Food and Drug Administration guidelines, including patient consent where appropriate. For more information, visit the Author Center.

Manuscript received August 3, 2022; revised manuscript received December 16, 2022, accepted December 19, 2022.

JACC: BASIC TO TRANSLATIONAL SCIENCE VOL. 8, NO. 6, 2023
JUNE 2023:702–719

(scAAV9)-based gene therapy vectors to the murine CLTI limb. We hypothesized that strategies with lower injection volumes and higher viral titers would produce the greatest levels of viral infection with minimal side-effects stemming from the injection. Next, we used the most effective scAAV9 treatment strategy for CLTI to examine the potential therapeutic effects of insulin-like growth factor (IGF)-1, which is known to promote muscle hypertrophy and enhance regeneration from injury in non-CLTI conditions.[29-31] We hypothesized that PAD/CLTI mice treated with scAAV9-IGF-1 would exhibit improved limb recovery compared with scAAV9-green fluorescent protein (GFP) controls.

METHODS

ANIMALS. Experiments were conducted on 8- to 10-week-old BALB/cJ male and female mice (n = 56) purchased from Jackson Laboratories (strain no. 000651). All mice were housed in a temperature (22 °C) and light (12 h light/12 h dark) controlled room and maintained on standard chow diet (Envigo Teklad Global 18% Protein Rodent Diet 2918 irradiated pellet) with free access to food and water. All animal experiments adhered to the Guide for the Care and Use of Laboratory Animals from the Institute for Laboratory Animal Research, National Research Council, Washington, DC (National Academy Press). All procedures were approved by the Institutional Animal Care and Use Committee of the University of Florida (protocol no. 202010121).

ANIMAL MODEL OF PAD/CLTI. Femoral artery ligation (FAL)[32] was performed by anesthetizing mice with intraperitoneal injection of ketamine (90 mg/kg) and xylazine (10 mg/kg) and surgically inducing unilateral hindlimb ischemia by placing ligations on the femoral artery just distal of the inguinal ligament and immediately proximal to the saphenous and popliteal branches. Because most female patients with PAD/CLTI are older in age and postmenopausal, female mice underwent bilateral oophorectomy 7 to 10 days before FAL. Buprenorphine (0.05 mg/kg) was given postoperatively for analgesia. Limb necrosis was scored on the following scale: grade 0, no necrosis in ischemic limb; grade I, necrosis limited to toes; grade II, necrosis extending to dorsum pedis; grade III, necrosis extending to crus.

AAV PLASMID CONSTRUCTION. All experiments herein were performed using self-complimentary (sc) AAV vectors. The scAAV-cytomegalovirus (CMV)-GFP plasmid was purchased from Cell Biolabs (cat. no. AAV410). The IGF1 coding sequence was polymerase chain reaction (PCR) amplified (CloneAmp; Takara Bio, cat. no. 639298) from cDNA generated from a rat gastrocnemius muscle. The scAAV-CMV-GFP plasmid was digested with EcoRI and HpaI (New England Biolabs, cat. nos. R3101 and R0105) and the linearized scAAV-CMV plasmid without the GFP was gel purified. The rat IGF1 coding sequence was then inserted into the linearized scAAV-CMV plasmid with the use of In-Fusion cloning (Takara Bio, cat. no. 639650). The resulting plasmids for scAAV-CMV-GFP and scAAV-CMV-IGF1 were packaged with the use of AAV2/9 serotype by Vector Biolabs.

AAV DELIVERY TO THE CLTI LIMB. scAAV9 was delivered via intramuscular injections of the hindlimb gastrocnemius, tibialis anterior (TA), extensor digitorum longus (EDL), and flexor digitorum brevis (FDB) muscles 7 days after FAL surgery. To determine the optimal scAAV9 dosage and volume for the CLTI limb, 4 injection strategies were compared with a sham injection (insertion of needle without injection) as shown in Figure 1A. Mice were randomized to treatment groups at the time of injection based on limb necrosis scores. Experimenters responsible for performing all outcomes measures were blinded to the treatment group of the mice. Female animals received the same virus dosage, but the injection volume was decreased based on the percentage difference in muscle weights compared with males as follows: TA: 25 μL; EDL: 12 μL; gastrocnemius: 46 μL; FDB: 8 μL.

ASSESSMENT OF LIMB PERFUSION WITH LASER DOPPLER. Limb perfusion was measured with the use of a laser Doppler flowmeter (moorVMS-LDF, Moor Instruments) before and immediately after FAL surgery as well as weekly to 35 days after the FAL surgery. Under ketamine/xylazine anesthesia, the mice were placed on a water-circulating pad at 37 °C, and the leg hair was shaved with the use of a pen trimmer. Once the mouse's breathing pattern was stable, the laser Doppler probe was placed against the skin of the plantar skin proximal to the footpad, the mid-belly of the TA muscle, and the mid-belly of the lateral side of the gastrocnemius muscle to access the peripheral tissue blood flow. The data were collected for 30 seconds, and the average perfusion flux values were calculated. Limb perfusion was presented as a percentage of the nonischemic contralateral limb.

ASSESSMENT OF HINDLIMB GRIP STRENGTH. Unilateral hindlimb grip strength was measured using a Grip Strength Test Instrument (Bioseb; model no. BIO-GS3) before FAL surgery and 35 days after

FIGURE 1 Establishment of the Optimal AAV Dosing and Delivery Strategy for the Critically Ischemic Limb

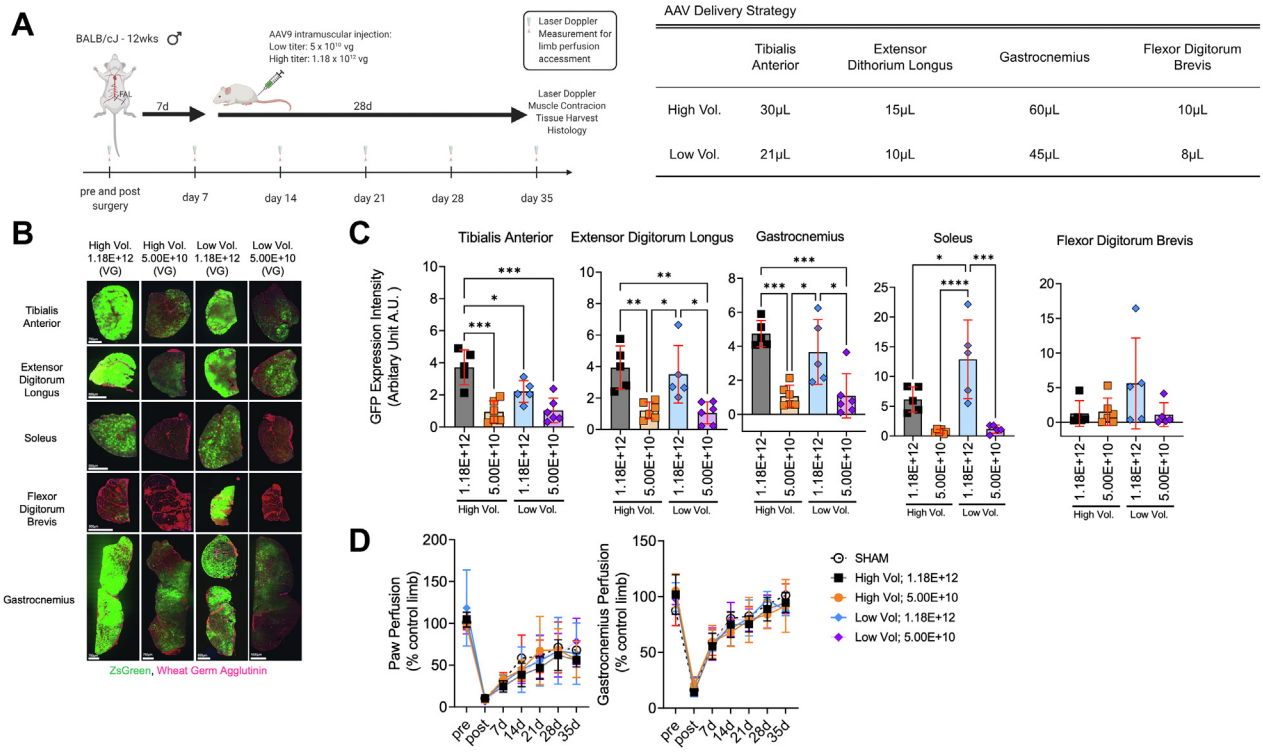

(A) Graphic abstract of study design and adeno-associated virus (AAV) injection volumes and titers (viral genomes [vg]), created with Biorender.com. FAL = femoral artery ligation. **(B)** Representative images of tibialis anterior, extensor digitorum longus, soleus, flexor digitorum brevis, and gastrocnemius muscles injected with self-complimentary (sc) AAV9--cytomegalovirus-green fluorescent protein (GFP) (n = 5-6/group) 35 days after FAL surgery. **(C)** Quantification of the GFP expression intensity (integral of area and intensity) across ischemic hindlimb muscles (n = 5-6/group). **(D)** Laser Doppler paw and gastrocnemius muscle perfusion recovery (n = 3-6/group). **Error bars** represent SD. **C**: 1-way ANOVA with Tukey's post hoc test; **D**: repeated-measures ANOVA. *$P < 0.05$; **$P < 0.01$; ***$P < 0.001$; ****$P < 0.0001$.

surgery. The mice were allowed to firmly grip the metal T-bar and the mice were pulled backward horizontally with increasing force until release of the T-bar. Three trials were performed per limb with 30 seconds of rest between each trial, and the highest force was recorded.

NERVE-MEDIATED MUSCLE CONTRACTILE FUNCTION. The maximal twitch and tetanic force levels of the TA muscle were measured in situ using stimulation of the sciatic nerve as previously described.[33] Briefly, the TA tendon was tied with a 4-0 silk suture attached to the lever arm of the force transducer (Cambridge Technology, model no. 2250). Muscle contractions were elicited by stimulating the sciatic nerve via bipolar electrodes using square wave pulses of 0.02 ms (701A stimulator, Aurora Scientific). Data collection and servomotor control were manipulated using a Lab-View-based DMC program (version 5.500). TA muscles were stretched to the optimal length first. Next, 3 isometric tetanic forces were acquired using a train of 150-Hz 500-ms supramaximal electrical pulses at the optimal length in the muscle, and the highest force among the 3 measurements was recorded as the peak tetanic force. One minute of rest was provided between each tetanic contraction. After tetanic contractions, 3 isometric twitch contractions (1 Hz) were performed, and the highest force was recorded as the peak twitch force.

SKELETAL MUSCLE HISTOLOGY AND IMMUNOFLUORESCENCE MICROSCOPY. Skeletal muscle morphology was assessed with the use of hematoxylin and eosin (H&E) staining and standard light microscopy as previously described.[34] Skeletal myofiber cross-sectional area (CSA), perfused capillary density, total capillary density, and satellite cell ($Pax7^+$) number were assessed by means of immunofluorescence microscopy as previously described.[34,35] In brief, 10- to 12-µm-thick transverse sections were cut from TA, EDL, gastrocnemius, soleus, and FDB muscles. For myofiber CSA analysis, muscle sections were

JACC: BASIC TO TRANSLATIONAL SCIENCE VOL. 8, NO. 6, 2023
JUNE 2023:702–719

FIGURE 2 AAV Injection Does Not Alter Myofiber Size or Histopathology in Critically Ischemic Muscle

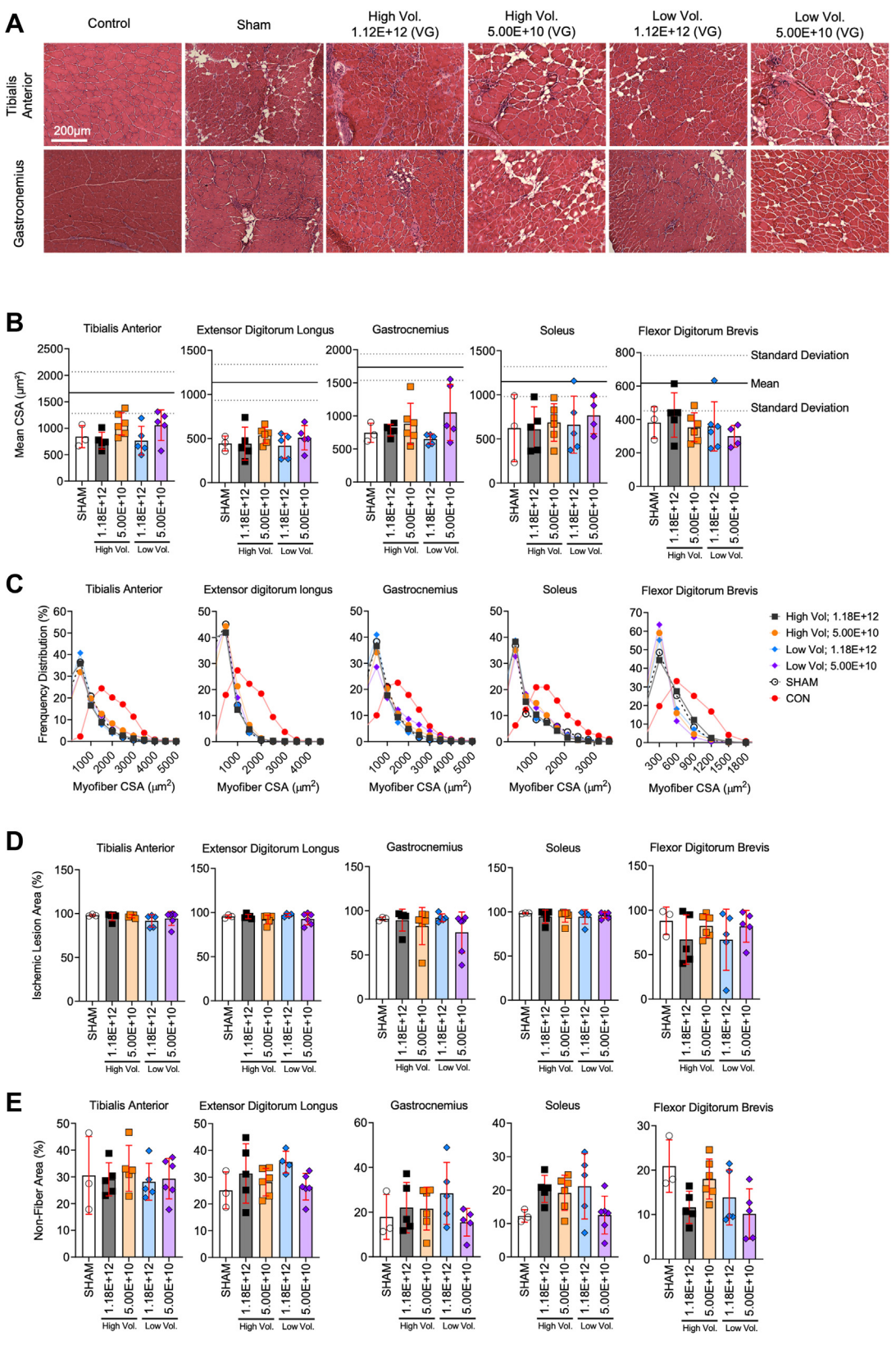

Continued on the next page

fixed with 4% paraformaldehyde (in phosphate-buffered saline solution [PBS]) for 5 minutes at room temperature followed by 30 minutes of incubation with Alexa647-conjugated wheat germ agglutinin (ThermoFisher Scientific, cat. no. W32466, 1:200 dilution) or overnight incubation at 4 °C with a primary antibody for laminin (Millipore-Sigma, cat. no. L9393, 1:100 dilution) followed by Alexa-Fluor secondary antibody incubation (ThermoFisher Scientific; cat. no. A21428, 1:250 dilution). For total capillary density analysis, muscle sections were incubated overnight (4 °C) with primary antibodies for laminin (Millipore-Sigma, cat. no. L9393, 1:200 dilution) and CD31 (Abcam, cat. no. ab7388, 1:200 dilution), subsequently washed with PBS, and then incubated with Alexa-Fluor secondary antibodies (ThermoFisher Scientific cat. no. A21434, 1:500 dilution, and cat. no. A32733, 1:500 dilution) for 1 hour at room temperature. To determine satellite cell content, muscle sections were incubated for 10 minutes in 100 mmol/L Glycine (Millipore-Sigma, cat. no. G8898) in PBS at room temperature for antigen retrieval, followed by 1 hour in a mouse-on-mouse blocking reagent (Vector Laboratories; cat. no. MKB-2213) and 1 hour in blocking buffer (5% goat serum, 2% bovine serum albumin, 0.1% Triton X-100, and 0.1% sodium azide in PBS) at room temperature. Next, muscle sections were incubated overnight (4 °C) with primary antibodies for Pax7 (DSHB; cat. no. PAX7, 1:300 dilution) and laminin (Millipore-Sigma, cat. no. L9393, 1:1,000 dilution). The next morning, slides were washed with PBS and incubated for 1 hour at room temperature with Alexa-Fluor secondary antibodies (ThermoFisher Scientific, cat. no. A21124, 1:1,000 dilution and ThermoFisher Scientific, cat. no. A21244, 1:1,000 dilution) and 6-diamino-2-phenylindole (Millipore-Sigma, cat. no. D9542, 1:1,000 dilution) and subsequently mounted in Fluoromount Mounting Medium (Millipore-Sigma, cat. no. F4680) and sealed for imaging. Images were obtained at ×20 magnification with the use of Evos FL2 Auto (ThermoFisher Scientific), and tiled images of the entire muscle were used for analysis. 50 μL *Griffonia simplicifolia* I isolectin B4 (Vector Laboratories; cat. no. DL1207) was given to mice through a retro-orbital injection and allowed to circulate systemically for 90 minutes to label perfused capillaries. All images were coded, and analysis was performed by blinded investigators. The level of GFP infection was quantified with the use of Image J as the integral of the area and fluorescence intensity obtained by manually circling the entire muscle. Myofiber CSAs were quantified with the use of the Muscle J program on laminin- and wheat-germ agglutinin–stained muscle sections.[36] With the use of Image J, the numbers of perfused and total ($CD31^+$) capillaries were measured by manual counting of fluorescence-positive vessels within the entire muscle section. Satellite cell density was measured by manual counting of $Pax7^+$ nuclei in 4 to 10 randomly selected ×20 images (number of images varied due to differences in size of the ischemic gastrocnemius and tibialis muscles). The nonmyofiber area of the skeletal muscle was quantified by manually adjusting the threshold of the H&E staining images to identify and measure the area of nonmyofiber tissue within the muscle section. The ischemic lesion area was quantified by manually tracing areas within the muscle section that showed clear signs of ischemic injury (ie, necrotic fibers, centralized nuclei, infiltrating mononuclear cells) with the use of H&E images in Image J. The percentage of myofibers with centralized nuclei were quantified by manually counting of fibers in 6 randomly selected ×20 images per muscle section for the nonsurgical limb and in the entire muscle section in the surgical limb.

RNA ISOLATION AND QUANTITATIVE REAL-TIME PCR. Total RNA was extracted from gastrocnemius muscle using TRIzol (Invitrogen; cat. no.15596018). The muscle sample was homogenized with the use of Trizol with PowerLyzer 24 (Qiagen), and RNA was isolated with the use of the Direct-zol RNA MiniPrep kit (Zymo Research, cat. no. R2052) according to the manufacturer's direction. RNA quantity and quality was assessed as previously described.[37] cDNA was generated from 200 ng RNA with the use of PrimeScript RT reagent kit with gDNA Eraser (Takara Bio; cat. no. RR047A) according to the manufacturer's directions. Real-time PCR was performed on a Quantstudio 3 (ThermoFisher Scientific) with the use of GoTaq qPCR Master Mix (Promega, cat. no. A6001) and Sybr Green primers for rat-IGF1

FIGURE 2 Continued

(A) Representative hematoxylin-eosin images of tibialis anterior and gastrocnemius muscles injected with scAAV9-CMV-GFP. **(B)** Quantification of mean myofiber area of hindlimb muscles (n = 3-6/group). The solid line represents the mean and dotted lines the SD of nonischemic muscle. **(C)** Histograms showing distribution of myofiber in hindlimb muscles. **(D)** Quantification of the ischemic lesion area (percentage of muscle injured). **(E)** Quantification of nonfiber area (percentage of total muscle area). **Error bars** represent SD. **B, D, and E**: 1-way ANOVA with Tukey's post hoc test. Abbreviations as in Figure 1.

FIGURE 3 Muscle Function Was Unaffected by Delivery of AAV to Critically Ischemic Muscle

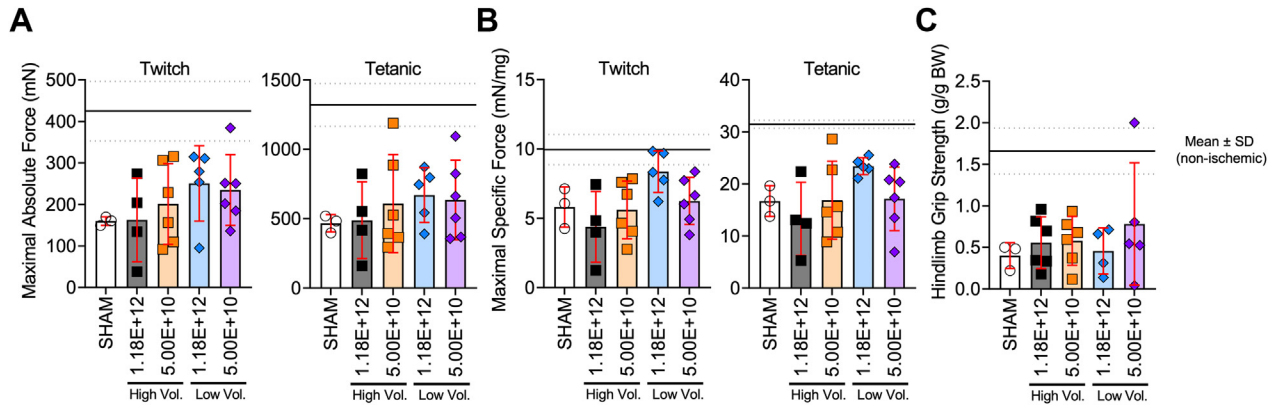

(A) Maximal absolute twitch and tetanic force of the ischemic tibialis anterior muscle stimulated via the sciatic nerve (n = 3-6/group). **(B)** Maximal specific twitch and tetanic force of the ischemic tibialis anterior muscle stimulated via the sciatic nerve (n = 3-6/group). **(C)** Hindlimb grip strength (normalized to body weight [BW]) measured 35 days after surgery (n = 3-6/group). The **solid lines** represent the mean and **dotted lines** the SD of nonischemic muscle. **Error bars** represent SD. 1-way ANOVA with Tukey's multiple comparison test. Abbreviations as in Figure 1.

(forward 5′-CTACAAAGTCAGCTCGTTCCA-3′, reverse 5′-TCTTGTTTCCTGCACTTCCTC-3′; Integrated DNA Technologies) and mouse-IGF1R (forward 5′- AGGAGAAGCCCATGTGTGAG-3′, reverse 5′-GTGTTGTCGTCCGGTGTGT-3′; Integrated DNA Technologies). β-Actin (forward 5′-GGCTGTATTCCCCTCCATCG-3′, reverse 5′-CCAGTTGGTAACAATGCCATGT-3′; Integrated DNA Technologies) was used as the housekeeping gene. Relative gene expression was calculated using $2^{-\Delta\Delta CT}$ from the GFP control group.

SERUM IGF-BINDING PROTEIN 3 CONTENT. Serum insulin-like growth factor-binding protein 3 (IGFBP3) levels were measured with the use of a mouse IGFBP3 enzyme-linked immunosorbent assay kit (R&D Systems, cat. no. MGB300), according to the manufacturer's instruction. Samples were measured in duplicate and the results were averaged and expressed in ng/mL.

STATISTICAL ANALYSIS. Data are presented as mean ± SD. Normality of data was tested with the Shapiro-Wilk test and visual inspection of QQ-plots. Experiments comparing scAAV9 dosage and volumes were analyzed with the use of 1-way analysis of variance (ANOVA) with Tukey's post hoc test. Laser Doppler perfusion recovery data were analyzed by means of repeated-measures ANOVA. Comparisons between scAAV9-GFP and scAAV9-IGF-1 were performed with the use of 2-way ANOVA with Šidák's post hoc test when interactions were detected. Differences in limb necrosis were analyzed using a Mann-Whitney *U*-test. All statistical analysis was performed with the use of GraphPad Prism (version 9.0), except for Mann-Whitney *U*-tests with the use of Vasserstats.net. In all cases, $P < 0.05$ was considered to be statistically significant.

RESULTS

OPTIMIZATION OF DOSAGE AND VOLUME FOR AAV DELIVERY TO THE CRITICALLY ISCHEMIC LIMB. The first goal of this study was to determine the the appropriate AAV dosage and injection volume to effectively transduce the critically ischemic limb without adverse impact on the limb health. To do this, 4 injection strategies using different injection volumes and viral dosage were compared as shown in Figure 1A. Importantly, AAVs were delivered to the hindlimb muscle 7 days after FAL, a time when the ischemic pathology is significant.[21,22,26,27,32] Quantification of the integral of the GFP intensity and area demonstrated a significant effect of viral titer ($P < 0.05$), with groups that received a higher AAV dosage (1.12×10^{12} viral genomes) having greater GFP infection (Figures 1B and 1C). In the majority of hindlimb muscles, there was no significant effect of injection volume on the GFP infection. Interestingly, the FDB muscle, located on the pad of the foot, proved to have poor infection regardless of titer or volume delivered. Importantly, neither AAV dosage nor volume altered perfusion recovery in the paw or gastrocnemius muscle compared with mice that received sham injections (insertion of the needle only) (Figure 1D).

FIGURE 4 Treatment With scAAV9-IGF-1 Significantly Reduced Limb Necrosis Progression in Female CLTI Mice

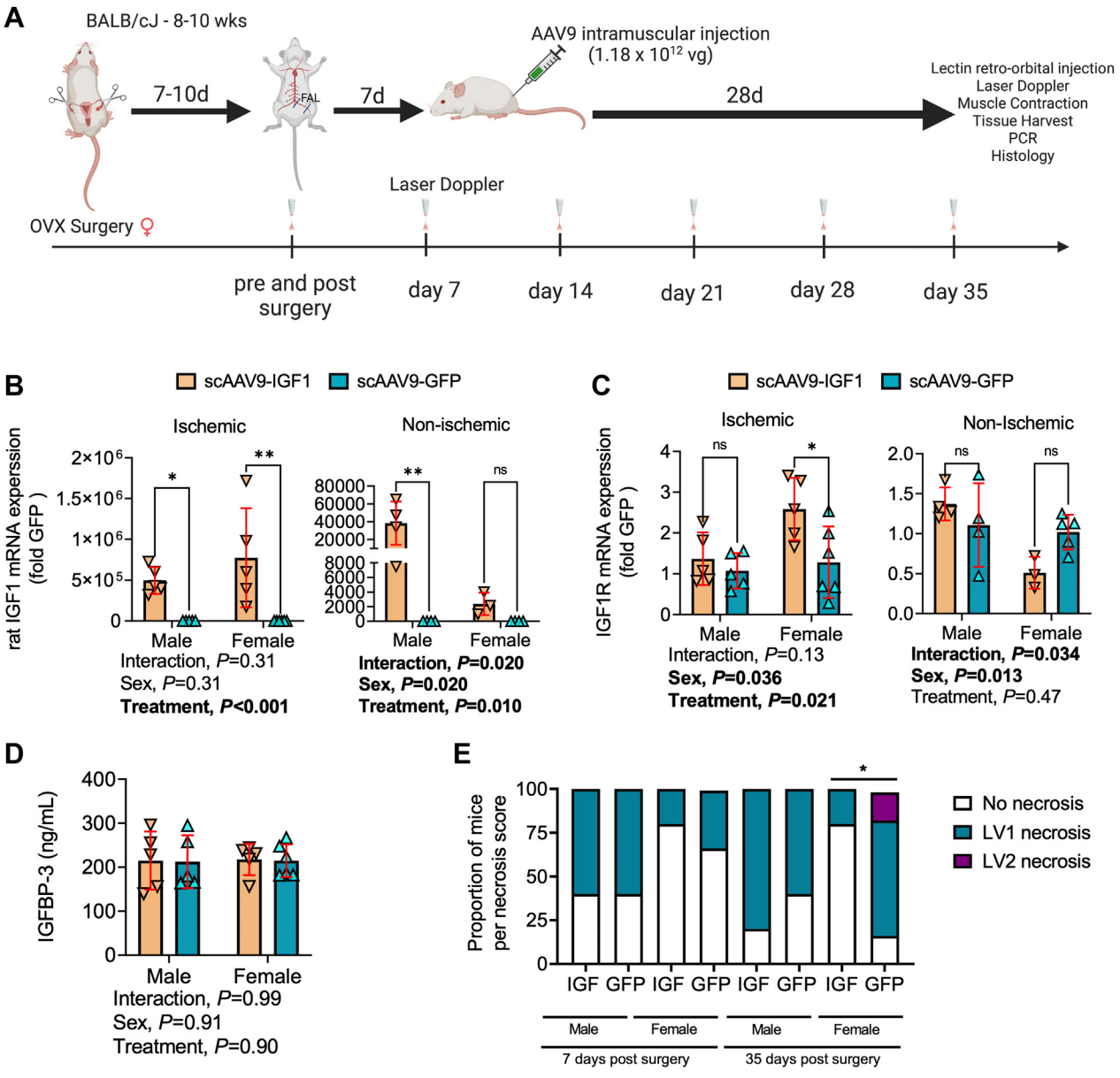

(A) Graphic abstract of study design, created with Biorender.com. OVX = ovariectomy. **(B)** mRNA levels of rat insulin-like growth factor (IGF)-1 in the ischemic and nonischemic gastrocnemius muscle (n = 3-6/group/sex). **(C)** mRNA levels of mice IGF1 receptor (IGF1R) in the ischemic and nonischemic gastrocnemius muscle (n = 3-6/group/sex). **(D)** Quantification of serum IGF-binding protein 3 (IGFBP3) concentration (n = 5-6/group/sex). **(E)** Distribution of limb necrosis scores at 7 and 35-days after FAL surgery (n = 5-6/group per sex). **Error bars** represent SD. **E**: Mann-Whitney *U*-test; **D to I**: 2-way ANOVA with Šidák's post hoc test when necessary. **P* < 0.05; ***P* < 0.01; ns = not significant. Abbreviations as in Figure 1.

AAV INJECTION DOSE DOES NOT ADVERSELY IMPACT MYOFIBER SIZE, HISTOPATHOLOGY, OR CONTRACTILE FUNCTION IN CRITICALLY ISCHEMIC MUSCLE. An assessment of safety is a crucial step for the development of new gene therapies in PAD/CLTI. As such, we investigated whether injection volume of dosing affected the muscle histopathology or function. Representative images of the limb muscles harvested at the time of death (35 days after FAL) are shown in Figure 2A. Compared with sham-injected muscles, scAAV9-GFP delivery did not affect the mean myofiber CSA (Figure 2B). Myofiber size

FIGURE 5 Treatment With scAAV9-IGF-1 Does Not Improve Perfusion Recovery or Capillary Density in the Critically Ischemic Limb

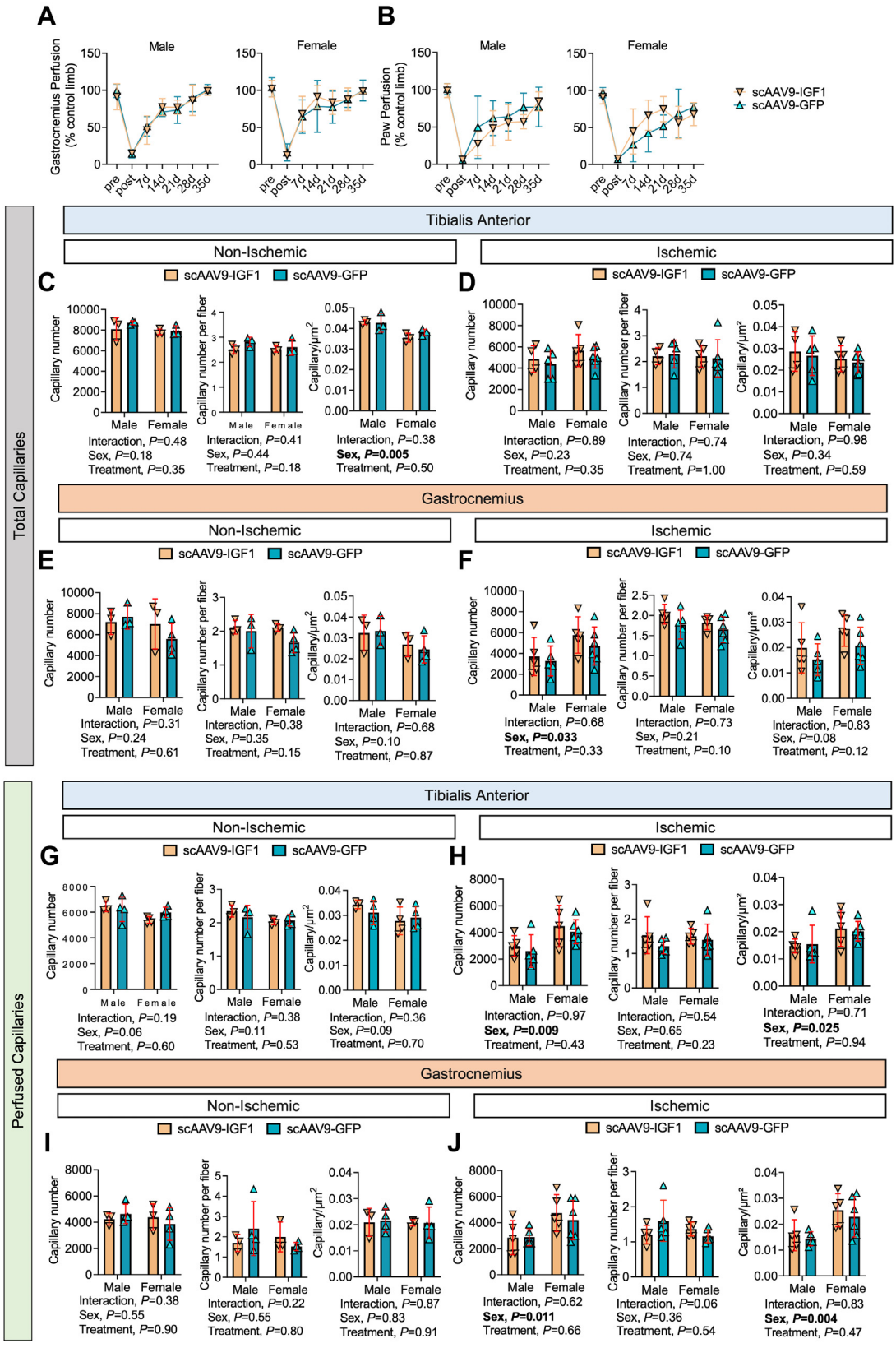

Continued on the next page

distributions, shown in Figure 2C, demonstrated a greater proportion of smaller myofiber sizes compared with non-ischemic control muscle. Similarly to the mean myofiber CSA, myofiber distributions in AAV-treated muscles were consistent with sham injected muscles. Furthermore, quantifications of the ischemic lesion area (amount of tissue with evidence of injury) and nonmyofiber areas were unaffected by AAV delivery (all $P > 0.05$) (Figures 2D and 2E). Because muscle function is an important contributor to PAD/CLTI pathophysiology, we also assessed muscle contractile function by means of nerve-mediated electrical stimulation of the tibialis anterior muscle. Compared with sham-injected mice, there were no significant differences in the maximal absolute (Figure 3A) or specific (Figure 3B) twitch or tetanic forces in mice that received scAAV9-GFP. Similarly, no differences in hindlimb grip strength were detected (Figure 3C).

TREATMENT WITH scAAV9-IGF-1 DOSE NOT IMPROVE PERFUSION RECOVERY OR CAPILLARY DENSITY IN THE CRITICALLY ISCHEMIC LIMB. Having established a strategy for delivery of AAV-based therapies to the critically ischemic murine limb that allows robust expression without adverse impact, the next step was to investigate the potential efficacy of a therapy. To this end, we chose to determine if treatment of the critically ischemic limb with IGF1 could improve ischemic limb pathology. IGF1 was chosen because of its well documented ability to promote muscle hypertrophy, enhance muscle regeneration after injury,[38,39] and induce angiogenesis.[40,41] Figure 4A illustrates the study design used to determine the therapeutic efficacy of scAAV9-IGF-1 treatment delivered to the critically ischemic limb. Analysis of IGF1 mRNA levels in the ischemic limb muscle levels confirmed significantly increased expression (Figure 4B). Interestingly, despite performing intramuscular injections only on the surgical limb, the contralateral control limb muscle also displayed an increase in IGF1 mRNA levels. This finding indicates that, despite low levels of limb perfusion at the time of injection, some AAV delivered intramuscularly can enter the circulation and reach tissues distant from the injection site. Furthermore, analysis of IGF1 receptor (IGF1R) uncovered a significant treatment effect ($P = 0.021$), with scAAV9-IGF-1 treated mice displaying higher levels of IGF1R mRNA (Figure 4C). Notably, this effect appeared to be stronger in female mice treated with scAAV9-IGF, which had a ~2.5-fold increase in IGF1R mRNA levels in the ischemic limb muscle. Serum IGFBP3 levels were not influenced by sex or treatment, indicating that systemic factors involved in IGF1 delivery were not altered in this study (Figure 4D).

Female mice that received scAAV9-IGF-1 treatment had significantly lower necrosis scores at the time of death compared with scAAV9-GFP-treated mice, indicating that IGF1 therapy may attenuate the progression of limb necrosis (Figure 4E). Laser Doppler measurements found no differences in the perfusion recovery of the gastrocnemius (Figure 5A) or paw (Figure 5B) between groups for both sexes. Consistent with this finding, scAAV9-IGF-1 had no impact on total capillary density (via CD31 immunolabeling treatment in either the control or ischemic TA (Figures 4C and 4D) or gastrocnemius (Figures 5E and 5F) muscles. Furthermore, in vivo labeling of perfused capillary density (via intravenous delivery of fluorescence-labeled *Griffonia simplicifolia* I isolectin) was also not affected by the treatment in either the control or ischemic TA (Figures 5G and 5H) or gastrocnemius (Figures 5I and 5J) muscles. Notably, there were some significant sex effects detected for the total and perfused capillary density, primarily in the ischemic muscles, indicating a more robust neovascularization response in female mice compared with male mice, regardless of treatment group (Figures 5F, 5H, and 5J).

TREATMENT WITH scAAV9-IGF-1 SIGNIFICANTLY INCREASED MUSCLE SIZE AND FORCE PRODUCTION IN THE CRITICALLY ISCHEMIC LIMB. Mice that received scAAV9-IGF-1 treatment had significantly larger (~36%) muscle mass in the TA ($P = 0.015$) and gastrocnemius ($P = 0.045$) muscles compared with mice that received scAAV9-GFP (Figure 6A). The EDLs were 26% and 33% larger in male and female scAAV9-IGF-1-treated mice, respectively, although the

FIGURE 5 Continued

(A) Gastrocnemius and **(B)** paw perfusion recovery (n = 5-6/group per sex). Quantification of total capillary number ($CD31^+$), total capillaries per myofiber, and total capillary number per muscle area (μm^2) within the **(C)** nonischemic and **(D)** ischemic tibialis anterior muscle and the **(E)** nonischemic and **(F)** ischemic gastrocnemius muscle (n = 3-6/group per sex). Quantification of perfused capillary number, perfused capillaries per myofiber, and perfused capillary number per muscle area (μm^2) within the **(G)** nonischemic and **(H)** ischemic tibialis anterior muscle and the **(I)** nonischemic and **(J)** ischemic gastrocnemius muscle (n = 3-6/group per sex). **Error bars** represent SD. **A and B**: repeated-measures ANOVA; **C to J**: 2-way ANOVA. Abbreviations as in Figure 1.

FIGURE 6 Treatment With scAAV9-IGF-1 Significantly Increases Muscle Size and Force Production in the Critically Ischemic Limb

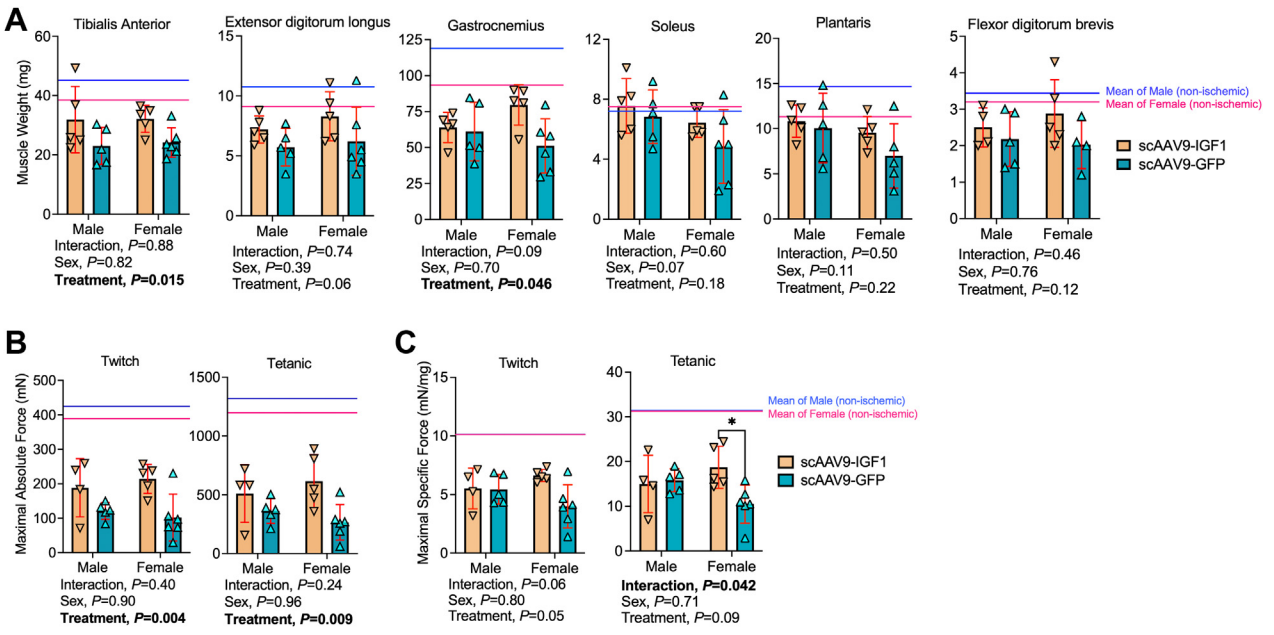

(A) Quantification of muscle weights in mice (n = 5-6/group per sex). **(B)** Maximal absolute twitch and tetanic force of the ischemic tibialis anterior muscle stimulated via the sciatic nerve (n = 4-6/group per sex). **(C)** Maximal specific twitch and tetanic force of the ischemic tibialis anterior muscle stimulated via the sciatic nerve (n = 4-6/group per sex). **Error bars** represent SD. Two-way ANOVA with Šidák's post hoc test when necessary. The **solid line** represents the mean values for nonischemic muscle in each sex (**blue** = male; **pink** = female). *$P < 0.05$. Abbreviations as in Figure 1.

treatment effect was not statistically significant ($P = 0.064$). The mass of deeper-lying plantar flexor muscles including the soleus and plantaris, as well as the FDB, were not different between groups. Functionally, there was a significant treatment effect for maximal absolute twitch ($P = 0.003$) and tetanic ($P = 0.008$) forces, establishing that scAAV-IGF1 improved muscle strength in mice with PAD/CLTI (Figure 6B). Interestingly, a significant interaction ($P = 0.042$) was detected in the maximal specific force (Figure 6C), but the treatment effect was nonsignificant ($P = 0.089$). Post hoc testing revealed that female mice treated with scAAV-IGF1 had significantly greater specific force levels compared with scAAV9-GFP female mice ($P = 0.016$). A similar trend was observed in the maximal specific twitch forces, although the interaction was not statistically significant ($P = 0.068$).

To assess myofiber size and histopathology, H&E staining and immunofluorescence microscopy were performed on transverse sections of the TA and gastrocnemius muscles. Frequency distributions of myofiber CSA of the TA muscle are shown in Figure 7A. Consistent with muscle weight and absolute force production, a significant treatment effect was observed in the mean myofiber CSA for the TA muscle ($P = 0.029$) (Figure 7B). However, quantification of the nonmyofiber area, ischemic lesion area, and the percentage of fibers with centralized nuclei in the TA muscle at day 35 after FAL were not different between groups (Figures 7C and 7E). Representative images of the TA muscle from each group are shown in Figure 7F. Despite an increase in muscle weight, no treatment effect was detected in the ischemic gastrocnemius mean myofiber CSA ($P = 0.31$) (Figures 7G and 7H). However, a significant interaction was detected for the mean myofiber CSA ($P = 0.047$), and subsequent post hoc testing revealed a nonsignificant increase in myofiber CSA in female mice treated scAAV9-IGF-1 ($P = 0.068$). Similar interactions, but not treatment effects, were detected for the nonmyofiber area (Figure 6I), ischemic lesion area (Figure 7J), and centralized nuclei (Figure 7K) in the gastrocnemius muscle. Post hoc testing again revealed sex-dependent effects of scAAV9-IGF-1 therapy, with females having lower nonmyofiber ($P = 0.053$), ischemic lesion areas ($P = 0.006$), and centrally nucleated myofibers ($P = 0.008$) compared

FIGURE 7 **Impact of scAAV9-IGF-1 on Myofiber Size and Histopathology in the Critically Ischemic Limb**

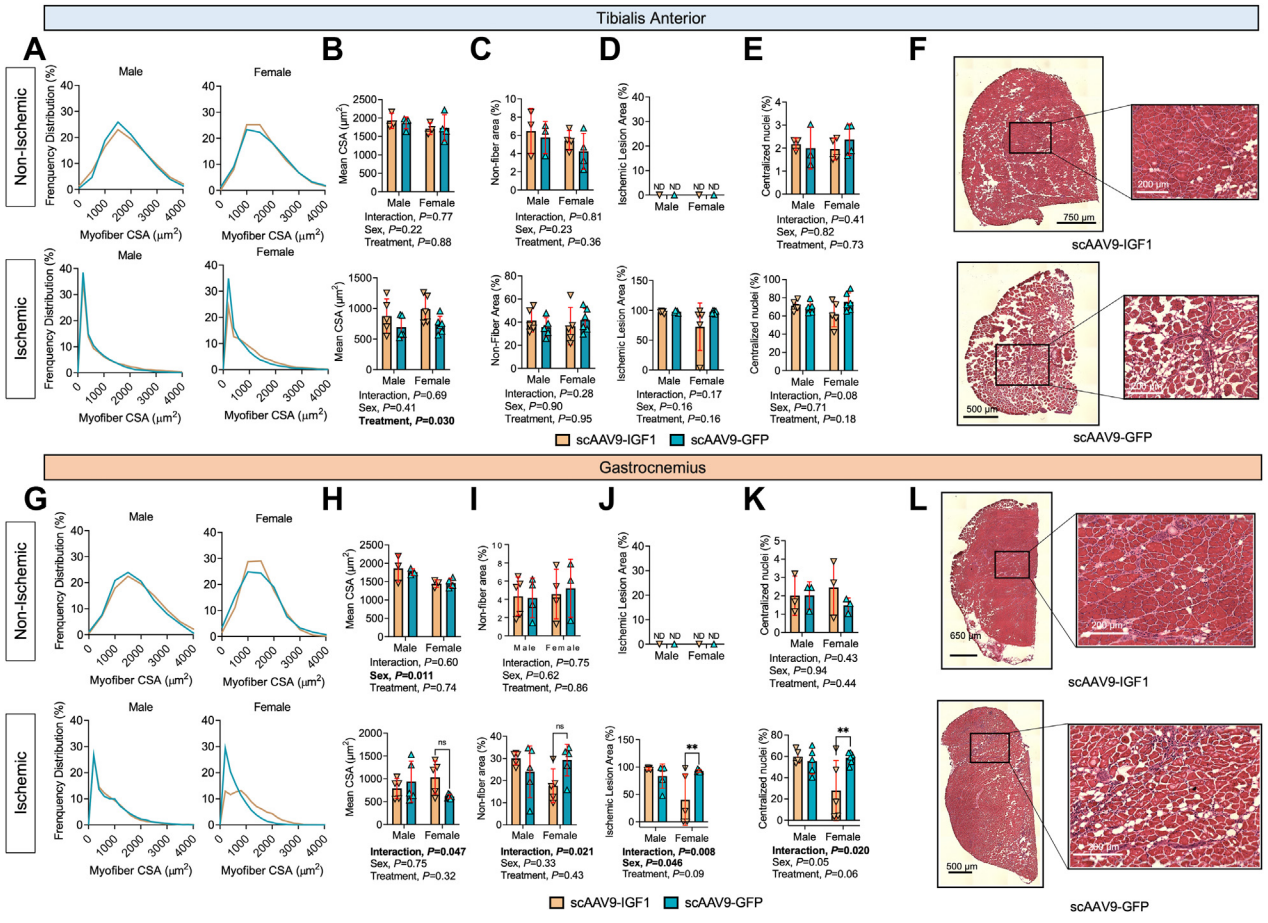

(A) Histograms of the distribution of myofiber cross-sectional area (CSA), **(B)** quantification of the mean myofiber area, **(C)** quantification of nonfiber area (percentage of total muscle area), **(D)** quantification of the ischemic lesion (percentage of muscle injured), and **(E)** quantification of the percentage of myofibers with centralized nuclei within the tibialis anterior muscles (n = 3-6/group per sex). **(F)** Representative hematoxylin-eosin images of tibialis anterior muscles in female mice. **(G)** Histograms of the distribution of myofiber CSA, **(H)** Quantification of the mean myofiber area, **(I)** Quantification of nonfiber area (percentage of total muscle area), **(J)** Quantification of the ischemic lesion (percentage of muscle injured), and **(K)** Quantification of the percentage of myofibers with centralized nuclei within the gastrocnemius muscles (n = 3-6/group per sex). **(L)** Representative hematoxylin-eosin images of lateral gastrocnemius muscles in female mice. **Error bars** represent SD. **B to E** and **H to K**: 2-way ANOVA with Šidák's post hoc test when necessary. $^{**}P < 0.01$; ns = not significant; nd = not determined. Abbreviations as in Figure 1.

with scAAV9-GFP-treated females. Representative images of the gastrocnemius muscles from the surgical limb are shown in Figure 7L.

To assess the impact of scAAV9-IGF-1 treatment on muscle regeneration, muscle sections were immunolabeled for Pax7 and satellite cell content was quantified in both nonischemic and ischemic TA and gastrocnemius muscles. These analyses revealed equivalent levels of satellite cells in both treatment groups, indicating that scAAV9-IGF-1 treatment did not affect satellite cell number, at least when measured 35 days after FAL and 28 days after treatment (Figure 8).

DISCUSSION

Compared with other acquired cardiovascular diseases, therapeutic development for the treatment of PAD/CLTI has been less than desirable. Medical management of PAD routinely involves treatments that reduce the risk of cardiovascular events, but the only medication approved specifically for the treatment PAD/CLTI is cilostazol, which was approved 1999. In the present study, we first established an effective and safe approach to deliver AAV-based gene therapy in an experimental model of severe PAD or CLTI. Using the most effective delivery

FIGURE 8 Treatment With scAAV9-IGF-1 Does Not Increase Pax7$^+$ Satellite Cell Density in the Critically Ischemic Limb

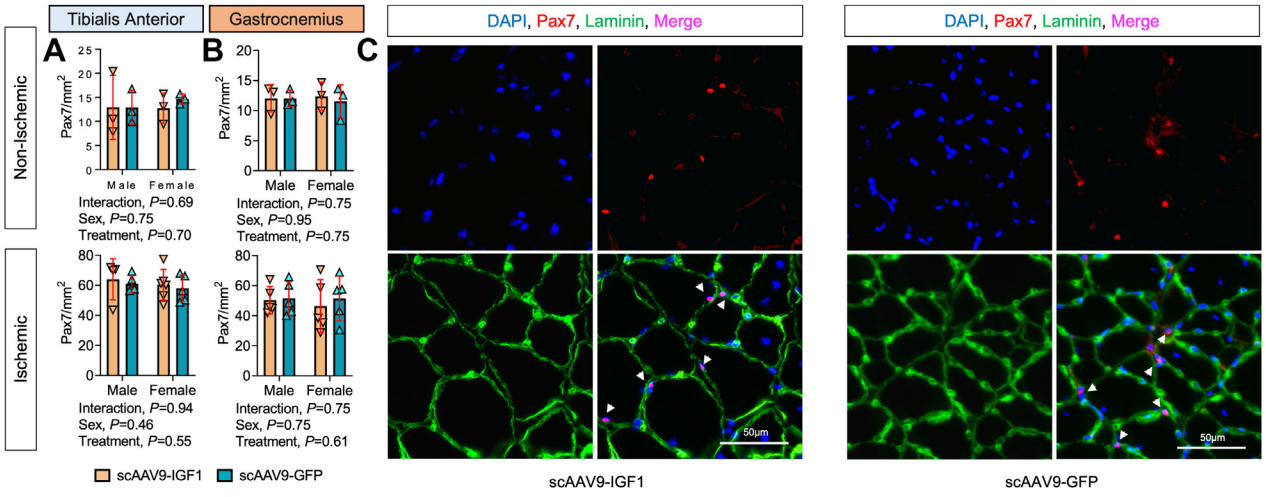

Quantification of the Pax7$^+$ cell number per muscle area (mm^2) within **(A)** the tibialis anterior muscle (n = 3-6/group per sex) and **(B)** the gastrocnemius muscle (n = 3-5/group per sex). **(C)** Representative immunofluorescence images of lateral gastrocnemius muscles from female mice in each treatment group. **Error bars** represent SD. **A and B**: 2-way ANOVA. Abbreviations as in Figure 1.

method, the therapeutic efficacy of a gene therapy encoding IGF1, a well-known growth factor that enhances myofiber regeneration,[42] was investigated. There are several noteworthy findings from this study. First, robust infection of the critically ischemic limb could be achieved with scAAV9 without adverse impact on limb pathophysiology. Second, treatment with scAAV9-IGF-1 did not improve perfusion recovery, total capillary density, or perfused capillary density in the critically ischemic limb. Third, treatment with scAAV9-IGF-1 significantly increased muscle size and absolute force production in the critically ischemic limb. Finally, treatment effects with scAAV9-IGF-1 displayed some sex-dependent effects, with female mice (but not males) having greater specific force and signs of improved histopathology in critically ischemic muscles.

In recent years, gene therapy has gained momentum owing to several treatments receiving regulatory approval for the treatment of human diseases. Many gene therapy clinical trials are currently underway or have been recently completed, covering a range of diseases including inflammatory, neurologic, cancer, infectious, and cardiovascular diseases.[43] Numerous cell- and gene-based therapies, primarily focused on stimulating vascular growth, have been tested in PAD/CLTI patients. Unfortunately, no such therapy has achieved success to date, and treatment options remain limited.[44] There are numerous factors that have likely contributed to the failed translation of PAD/CLTI therapies from preclinical research models to patients. First, PAD/CLTI patients often suffer from multiple comorbidities that accelerate disease pathogenesis and worsen outcomes. The interactions between the patient's individual genome, environment, and comorbidities are extremely difficult to model in a preclinical setting. Second, the primary focus of most PAD/CLTI gene- or cell-based therapies has been on stimulating blood vessel growth. Although this is undoubtedly an important goal, our understanding of the complex interactions between cell types within the PAD/CLTI limb required to achieve effective promotion of both blood vessel growth and regeneration of other injured cells (ie, muscle, nerve, skin) is incomplete. Moreover, the local microenvironment in the PAD/CLTI limb is quite different from that encountered in other pathologies, where gene- and cell-based therapies are having success, so PAD/CLTI-specific delivery strategies must be developed.

AAV has emerged as the leading platform for gene therapy in the treatment of human disease. Although generally considered to be safe and less immunogenic than other viral vectors, there is evidence that wild-type AAV exposure may contribute to production of neutralizing antibodies that may affect gene transfer.[45] In addition, the health of the recipient tissue may play a role in the efficacy of AAV gene transfer. In a recent study, Mollard et al[46] reported that AAV transduction was much lower in muscles regenerating

from either cardiotoxin injection or the effects of muscular dystrophy. This effect was observed when AAV treatment was applied both 3 and 45 weeks after cardiotoxin injury. This is a particularly relevant discovery for PAD/CLTI AAV therapies because the ischemic muscle is pathologic and shows histologic characteristics of regenerating muscle. In the present study, we established efficacious dosing and volumes for the delivery of scAAV9 to the CLTI limb. Robust expression of the GFP transgene was achieved across nearly all hindlimb muscles despite providing the AAV-therapy 7 days after FAL, when the tissue pathology in BALB/c mice is substantial.[21,22,25-27,32] Importantly, transgene delivery and expression had no adverse impact on limb perfusion recovery, muscle contractile function, or limb histopathology. In consideration of the need for rapid expression of AAV therapy in the PAD/CLTI limb, we used scAAVs to circumvent the need to synthesize the second strand of DNA before expression of the transgene.

Although the etiology of PAD/CLTI undoubtedly begins in the vasculature with impaired blood flow to the limb, muscle function and quality have been identified as major predictors of patient outcomes and quality of life.[47-52] Walking performance, as measured by the 6-minute walk distance, is widely used to evaluate therapeutic interventions in PAD.[53-55] A component of walking performance is related to muscular strength, power, and endurance. Various groups have documented pathologic abnormalities within the skeletal muscle of PAD patients with claudication and patients with CLTI.[56-63] Few clinical studies have used objective measures of muscle strength or power in CLTI patients, particularly in the context of randomized clinical trials. Cross-sectional studies have reported that patients with PAD are about 15% to 20% weaker than matched adults without PAD.[64,65] Furthermore, muscle mass and density and leg strength measures were reported to be strong predictors of outcomes in severe PAD/CLTI patients.[51,66,67] Two longitudinal observational studies in PAD patients with claudication reported that low muscle strength was associated with higher all-cause mortality.[52,68] Furthermore, one recent study reported a strong positive association between walking performance and calf muscle myofiber size.[69] Taken together, these findings suggest that therapies aimed to increase muscle size and strength may benefit patients with PAD/CLTI. It is difficult to directly compare our results of nerve-mediated contraction in mice with voluntary strength measures in patients. Nonetheless, some descriptive comparisons highlight both the severity of myopathy and the magnitude of therapeutic benefit of IGF1 that we observed. Compared with the nonsurgical limb, muscle force levels decreased by around 75% in the FAL limb of scAAV9-GFP mice, demonstrating a severe limb myopathy in those CLTI mice. Treatment with scAAV9-IGF-1 increased muscle force levels by 40% in males and 230% in females, demonstrating a considerable improvement in muscle function. Considering the magnitude of weakness in patients with PAD (~15%-20%), it is reasonable to hypothesize that the achievement of similar increases in muscle strength in human patients with PAD/CLTI may significantly improve limb function and quality of life.

Numerous studies have demonstrated that IGF1 can promote muscle protein synthesis, resulting in muscle hypertrophy.[70] IGF1 has been shown to enhance muscle regeneration from injury or disuse.[71-73] In addition to promotion of myogenesis, IGF1 has been proven to induce angiogenesis,[41,74] decrease atherosclerosis,[75,76] reduce degeneration of motor neurons,[77] and suppress inflammation.[75,76] In the present study, self-complimentary AAV9-IGF1 therapy significantly increased both muscle size (~36%) and strength in male and female mice with experimental PAD/CLTI (**Figure 5**). Interestingly, the therapeutic efficacy of scAAV9-IGF-1 was greater in female mice than in males. For example, male mice treated with scAAV9-IGF-1 had ~40% higher absolute muscle force compared with scAAV9-GFP controls, whereas female mice treated with scAAV9-IGF-1 had ~230% higher muscle force compared with controls. Notably, the observed increase in muscle strength occurred without improvements in perfusion recovery or capillary density (**Figure 4**). A study by Borselli et al[30] reported that treatment with alginate gels containing recombinant vascular endothelial growth factor (VEGF) and IGF1 could improve muscle regeneration and force levels after FAL. Similar to our results, that study reported that gels containing only IGF1 did not improve limb perfusion recovery. In contrast to our study, only mice that received a combination of VEGF and IGF1, but not those that received IGF1 alone, displayed greater muscle size (~25%) compared with controls. Unfortunately, that study reported muscle force/strength measures only for mice treated with VEGF+IGF1, so direct comparisons with the present study regarding efficacy of IGF1 treatment cannot be made. There are some noteworthy differences in experimental approach between the present study and that by Borselli et al.[30] First, the present study used male and female mice, whereas only females were used in the work by Borselli et al.[30] Moreover, female mice in the present study underwent oophorectomy to better

JACC: BASIC TO TRANSLATIONAL SCIENCE VOL. 8, NO. 6, 2023
JUNE 2023:702–719

mimic the postmenopausal condition of female patients with PAD. In addition, the present study used BALB/c mice, which experience more severe muscle injury, less perfusion recovery, and less angiogenesis after limb ischemia compared with C57BL/6 mice.[27,28] In addition, there are differences in both delivery method (alginate gel vs scAAV9) and timing (immediately after FAL vs 7 days after FAL) that contribute to a different local microenvironment at the time of treatment.

In the present study, we uncovered some unexpected sex differences regarding the efficacy of the IGF1 treatment in the critically ischemic limb. As discussed above, the relative improvement in muscle strength in female mice was approximately 5 times greater than in male mice treated with scAAV9-IGF-1. In the ischemic gastrocnemius muscle, female (but not male) mice treated with scAAV9-IGF-1 had lower ischemic lesion areas, number of fibers with centralized nuclei, and nonmyofiber areas compared with scAAV9-GFP control mice. There are several factors that could explain the sex-dependent efficacy differences. First, we unexpectedly observed that female mice treated with scAAV9-IGF-1 also displayed significantly higher mRNA levels of the endogenous IGF1 receptor compared with control mice (**Figure 4C**). Second, estradiol has been shown to rapidly activate the IGF1 receptor,[78] as well as to stimulate hepatic IGF1 production,[79] demonstrating coupling between the estrogen and IGF1 signaling pathways. Female mice in this study had their ovaries removed 7 to 10 days before FAL surgery, which reduces estradiol levels. Furthermore, estradiol has also been linked to growth hormone levels,[80] which is known to stimulate hepatic IGF1 production. As recently reviewed by McMillin et al,[81] disruptions in sex-hormone levels, including deficiencies in estradiol, have been linked to an accelerated loss of skeletal muscle. Thus, the oophorectomy procedure likely makes female mice more vulnerable to ischemic myopathy. This statement is partially supported by our recent study in female BALB/c mice without oophorectomy, where the loss of muscle force was ~50% in the FAL limb,[82] compared with the ~70% decrease in muscle force reported in the present study with oophorectomized female BALB/c mice. Taken together, these findings could explain the greater efficacy of scAAV9-IGF-1 in female mice that we observed in the present study. More importantly, the present results highlight the critical need for adequate female representation in clinical trials enrolling patients with PAD/CLTI and the necessity for thorough statistical analysis of sex-dependent treatment efficacies.

STUDY LIMITATIONS. There are some limitations of the experimental approaches used in this study. First, this study used younger mice, despite the widely known increase in PAD prevalence with increasing age. Younger mice were used owing to the difficulties in obtaining aged mice, especially for strains such as BALB/c, where aged colonies are not available from commercial or public vendors. Furthermore, patients with PAD/CLTI often suffer from numerous comorbid conditions, such as hypertension, diabetes, renal disease, and hyperlipidemia, that were not present in the mice used in this study. These comorbidities, coupled with genetic and environmental (eg, smoking, poor diet, lack of physical activity) risk factors are incredibly challenging to replicate in preclinical research. In addition, PAD/CLTI is typically a progressive disease by which atherosclerosis develops slowly over time. In contrast, a rapid and severe loss of limb blood was induced by means of FAL in the present study. Experiments in this study delivered a foreign protein (GFP) to determine infectivity and as a control group in comparisons with IGF1-treated mice. Detailed examination of potential toxic or immune responses to the presence of GFP were not performed in this study, although comparisons of muscle histopathology and contractile function did not indicate adverse impact compared with sham-injected animals (**Figures 2 and 3**).

CONCLUSIONS

We have provided an in-depth validation of viral infection and assess its safety in mice with experimental PAD/CLTI. Furthermore, we established the potent therapeutic efficacy of scAAV9-IGF-1 in an experimental model of PAD/CLTI which improved both muscle size and strength. Finally, we unexpectedly uncovered sex differences in the effectiveness of IGF1 therapy, with female mice exhibiting more powerful improvements in limb function compared with male mice.

FUNDING SUPPORT AND AUTHOR DISCLOSURES

This study was supported by National Institutes of Health (NIH) grant R01-HL149704 (to Dr Ryan). Dr Kim was supported by American Heart Association grant POST903198. Mr Thome was supported by NIH grant F31-DK128920. All other authors have reported that they have no relationships relevant to the contents of this paper to disclose.

ADDRESS FOR CORRESPONDENCE: Dr Terence E. Ryan, University of Florida, 1864 Stadium Road, Gainesville, Florida 32611, USA. E-mail: ryant@ufl.edu. Twitter: @TerenceRyan_PhD.

PERSPECTIVES

COMPETENCY IN MEDICAL KNOWLEDGE: Although skeletal muscle pathophysiology has emerged as a key factor in PAD outcomes, current medical therapies are not directed toward improving limb function. In this study, we established a safe and effective strategy for delivering AAV-based therapies to the limb muscle in a rodent model of severe PAD/CLTI. Treatment with self-complimentary AAV9-IGF1 was found to significantly increase muscle size and strength in PAD/CLTI mice.

TRANSLATIONAL OUTLOOK: This study demonstrates that therapies aimed to rescue skeletal myopathy in PAD/CLTI can significantly improve limb function and enhance regenerative ability. Unexpectedly, female mice were found to respond to IGF1 therapy more favorably than male mice. These findings suggest that robust and well controlled studies in human PAD/CLTI should explore the therapeutic potential of IGF1 therapy, but careful consideration of biological sex is necessary.

REFERENCES

1. Conte SM, Vale PR. Peripheral arterial disease. *Heart Lung Circ*. 2018;27:427–432.

2. Go AS, Mozaffarian D, Roger VL, et al. Heart disease and stroke statistics—2014 update: a report from the American Heart Association. *Circulation*. 2014;129:e28–e292.

3. Fowkes FG, Rudan D, Rudan I, et al. Comparison of global estimates of prevalence and risk factors for peripheral artery disease in 2000 and 2010: a systematic review and analysis. *Lancet*. 2013;382:1329–1340.

4. Novo S, Coppola G, Milio G. Critical limb ischemia: definition and natural history. *Curr Drug Targets Cardiovasc Haematol Disord*. 2004;4:219–225.

5. Kim K, Anderson EM, Scali ST, Ryan TE. Skeletal muscle mitochondrial dysfunction and oxidative stress in peripheral arterial disease: a unifying mechanism and therapeutic target. *Antioxidants (Basel)*. 2020;9.

6. Conte MS, Bradbury AW, Kolh P, et al. Global vascular guidelines on the management of chronic limb-threatening ischemia. *Eur J Vasc Endovasc Surg*. 2019;58(1 suppl):S1–S109.e33.

7. Tsai TT, Rehring TF, Rogers RK, et al. The contemporary safety and effectiveness of lower extremity bypass surgery and peripheral endovascular interventions in the treatment of symptomatic peripheral arterial disease. *Circulation*. 2015;132:1999–2011.

8. Taylor SM, Kalbaugh CA, Blackhurst DW, et al. Determinants of functional outcome after revascularization for critical limb ischemia: an analysis of 1000 consecutive vascular interventions. *J Vasc Surg*. 2006;44:747–755. discussion 755–756.

9. Deguchi J, Shigematsu K, Ota S, Kimura H, Fukayama M, Miyata T. Surgical result of critical limb ischemia due to tibial arterial occlusion in patients with systemic scleroderma. *J Vasc Surg*. 2009;49:918–923.

10. Goodney PP, Beck AW, Nagle J, Welch HG, Zwolak RM. National trends in lower extremity bypass surgery, endovascular interventions, and major amputations. *J Vasc Surg*. 2009;50:54–60.

11. Hammer A, Steiner S. Gene therapy for therapeutic angiogenesis in peripheral arterial disease—a systematic review and meta-analysis of randomized, controlled trials. *Vasa*. 2013;42:331–339.

12. Rajagopalan S, Mohler ER, Lederman RJ, et al. Regional angiogenesis with vascular endothelial growth factor in peripheral arterial disease: a phase II randomized, double-blind, controlled study of adenoviral delivery of vascular endothelial growth factor 121 in patients with disabling intermittent claudication. *Circulation*. 2003;108:1933–1938.

13. Kusumanto YH, van Weel V, Mulder NH, et al. Treatment with intramuscular vascular endothelial growth factor gene compared with placebo for patients with diabetes mellitus and critical limb ischemia: a double-blind randomized trial. *Hum Gene Ther*. 2006;17:683–691.

14. Shishehbor MH, Rundback J, Bunte M, et al. SDF-1 plasmid treatment for patients with peripheral artery disease (STOP-PAD): randomized, double-blind, placebo-controlled clinical trial. *Vasc Med*. 2019;24:200–207.

15. Shimpo M, Ikeda U, Maeda Y, et al. AAV-mediated VEGF gene transfer into skeletal muscle stimulates angiogenesis and improves blood flow in a rat hindlimb ischemia model. *Cardiovasc Res*. 2002;53:993–1001.

16. Sugano M, Tsuchida K, Makino N. Intramuscular gene transfer of soluble tumor necrosis factor-alpha receptor 1 activates vascular endothelial growth factor receptor and accelerates angiogenesis in a rat model of hindlimb ischemia. *Circulation*. 2004;109:797–802.

17. Ishii M, Numaguchi Y, Okumura K, et al. Mesenchymal stem cell-based gene therapy with prostacyclin synthase enhanced neovascularization in hindlimb ischemia. *Atherosclerosis*. 2009;206:109–118.

18. Saqib A, Prasad KM, Katwal AB, et al. Adeno-associated virus serotype 9-mediated overexpression of extracellular superoxide dismutase improves recovery from surgical hind-limb ischemia in BALB/c mice. *J Vasc Surg*. 2011;54:810–818.

19. Palladino M, Gatto I, Neri V, et al. Combined therapy with sonic hedgehog gene transfer and bone marrow–derived endothelial progenitor cells enhances angiogenesis and myogenesis in the ischemic skeletal muscle. *J Vasc Res*. 2012;49:425–431.

20. Fang QZ, Mok PY, Thomas AE, et al. Pleiotrophin gene therapy for peripheral ischemia: evaluation of full-length and truncated gene variants. *PLoS One*. 2013;8.

21. McClung JM, McCord TJ, Ryan TE, et al. BAG3 (Bcl-2-associated athanogene3) coding variant in mice determines susceptibility to ischemic limb muscle myopathy by directing autophagy. *Circulation*. 2017;136:281–296.

22. Ryan TE, Schmidt CA, Tarpey MD, et al. PFKFB3-mediated glycolysis rescues myopathic outcomes in the ischemic limb. *JCI Insight*. 2020;5.

23. Thirunavukkarasu M, Rishi MT, Pradeep SR, et al. Heat shock protein A12B gene therapy improves perfusion, promotes neovascularization, and decreases fibrosis in a murine model of hind limb ischemia. *Surgery*. 2021;170:969–977.

24. Thirunavukkarasu M, Pradeep SR, Ukani G, et al. Gene therapy with Pellino-1 improves perfusion and decreases tissue loss in Flk-1 heterozygous mice but fails in MAPKAP Kinase-2 knockout murine hind limb ischemia model. *Microvasc Res*. 2022;141.

25. Dokun AO, Keum S, Hazarika S, et al. A quantitative trait locus (LSq-1) on mouse chromosome 7 is linked to the absence of tissue loss after surgical hindlimb ischemia. *Circulation*. 2008;117:1207–1215.

26. McClung JM, McCord TJ, Keum S, et al. Skeletal muscle-specific genetic determinants contribute to the differential strain-dependent effects of hindlimb ischemia in mice. *Am J Pathol*. 2012;180:2156–2169.

27. McClung JM, McCord TJ, Southerland K, et al. Subacute limb ischemia induces skeletal muscle injury in genetically susceptible mice independent of vascular density. *J Vasc Surg*. 2016;64:1101–1111.e2.

28. Schmidt CA, Amorese AJ, Ryan TE, et al. Strain-dependent variation in acute ischemic muscle injury. *Am J Pathol*. 2018;188:1246–1262.

29. Ye F, Mathur S, Liu M, et al. Overexpression of insulin-like growth factor-1 attenuates skeletal muscle damage and accelerates muscle regeneration and functional recovery after disuse. *Exp Physiol*. 2013;98:1038–1052.

30. Borselli C, Storrie H, Benesch-Lee F, et al. Functional muscle regeneration with combined delivery of angiogenesis and myogenesis factors. *Proc Natl Acad Sci U S A*. 2010;107:3287–3292.

31. Teng YC, Porfírio-Sousa AL, Ribeiro GM, et al. Analyses of the pericyte transcriptome in ischemic skeletal muscles. *Stem Cell Res Ther*. 2021;12:183.

32. Ryan TE, Schmidt CA, Alleman RJ, et al. Mitochondrial therapy improves limb perfusion and myopathy following hindlimb ischemia. *J Mol Cell Cardiol*. 2016;97:191–196.

33. Spinazzola JM, Smith TC, Liu M, Luna EJ, Barton ER. Gamma-sarcoglycan is required for the response of archvillin to mechanical stimulation in skeletal muscle. *Hum Mol Genet*. 2015;24:2470–2481.

34. Berru FN, Gray SE, Thome T, et al. Chronic kidney disease exacerbates ischemic limb myopathy in mice via altered mitochondrial energetics. *Sci Rep*. 2019;9:15547.

35. Yue F, Oprescu SN, Qiu JM, et al. Lipid droplet dynamics regulate adult muscle stem cell fate. *Cell Rep*. 2022;38.

36. Mayeuf-Louchart A, Hardy D, Thorel Q, et al. MuscleJ: a high-content analysis method to study skeletal muscle with a new Fiji tool. *Skelet Muscle*. 2018;8:25.

37. Salyers ZR, Coleman M, Balestrieri NP, Ryan TE. Indoxyl sulfate impairs angiogenesis via chronic aryl hydrocarbon receptor activation. *Am J Physiol Cell Physiol*. 2021;320:C240–C249.

38. Florini JR, Ewton DZ, Coolican SA. Growth hormone and the insulin-like growth factor system in myogenesis. *Endocr Rev*. 1996;17:481–517.

39. Duan C, Ren H, Gao S. Insulin-like growth factors (IGFs), IGF receptors, and IGF-binding proteins: roles in skeletal muscle growth and differentiation. *Gen Comp Endocrinol*. 2010;167:344–351.

40. Rabinovsky ED, Draghia-Akli R. Insulin-like growth factor I plasmid therapy promotes in vivo angiogenesis. *Mol Ther*. 2004;9:46–55.

41. Alcazar CA, Hu C, Rando TA, Huang NF, Nakayama KH. Transplantation of insulin-like growth factor-1 laden scaffolds combined with exercise promotes neuroregeneration and angiogenesis in a preclinical muscle injury model. *Biomater Sci*. 2020;8:5376–5389.

42. Yoshida T, Delafontaine P. Mechanisms of IGF-1-mediated regulation of skeletal muscle hypertrophy and atrophy. *Cells*. 2020;9.

43. Anguela XM, High KA. Entering the modern era of gene therapy. *Annu Rev Med*. 2019;70:273–288.

44. Ylä-Herttuala S. Gene therapy of critical limb ischemia enters clinical use. *Mol Ther*. 2019;27:2053.

45. Verdera HC, Kuranda K, Mingozzi F. AAV vector immunogenicity in humans: a long journey to successful gene transfer. *Mol Ther*. 2020;28:723–746.

46. Mollard A, Peccate C, Forand A, et al. Muscle regeneration affects adeno associated virus 1 mediated transgene transcription. *Sci Rep*. 2022;12:9674.

47. Pizzimenti M, Meyer A, Charles AL, et al. Sarcopenia and peripheral arterial disease: a systematic review. *J Cachexia Sarcopenia Muscle*. 2020;11:866–886.

48. Sugai T, Watanabe T, Otaki Y, et al. Decreased psoas muscle computed tomography value predicts poor outcome in peripheral artery disease. *Circ J*. 2018;82:3069–3075.

49. McDermott MM, Liu K, Ferrucci L, et al. Decline in functional performance predicts later increased mobility loss and mortality in peripheral arterial disease. *J Am Coll Cardiol*. 2011;57:962–970.

50. McDermott MM, Ferrucci L, Guralnik J, et al. Pathophysiological changes in calf muscle predict mobility loss at 2-year follow-up in men and women with peripheral arterial disease. *Circulation*. 2009;120:1048–1055.

51. Morris DR, Skalina TA, Singh TP, Moxon JV, Golledge J. Association of computed tomographic leg muscle characteristics with lower limb and cardiovascular events in patients with peripheral artery disease. *J Am Heart Assoc*. 2018;7.

52. Singh N, Liu K, Tian L, et al. Leg strength predicts mortality in men but not in women with peripheral arterial disease. *J Vasc Surg*. 2010;52:624–631.

53. Nayak P, Guralnik JM, Polonsky TS, et al. Association of six-minute walk distance with subsequent lower extremity events in peripheral artery disease. *Vasc Med*. 2020;25:319–327.

54. McDermott MM, Spring B, Tian L, et al. Effect of low-intensity vs high-intensity home-based walking exercise on walk distance in patients with peripheral artery disease: the LITE randomized clinical trial. *JAMA*. 2021;325:1266–1276.

55. Englund EK, Langham MC, Wehrli FW, et al. Impact of supervised exercise on skeletal muscle blood flow and vascular function measured with MRI in patients with peripheral artery disease. *Am J Physiol Heart Circ Physiol*. 2022.

56. Regensteiner JG, Wolfel EE, Brass EP, et al. Chronic changes in skeletal muscle histology and function in peripheral arterial disease. *Circulation*. 1993;87:413–421.

57. Pipinos II, Sharov VG, Shepard AD, et al. Abnormal mitochondrial respiration in skeletal muscle in patients with peripheral arterial disease. *J Vasc Surg*. 2003;38:827–832.

58. McDermott MM, Hoff F, Ferrucci L, et al. Lower extremity ischemia, calf skeletal muscle characteristics, and functional impairment in peripheral arterial disease. *J Am Geriatr Soc*. 2007;55:400–406.

59. Ryan TE, Yamaguchi DJ, Schmidt CA, et al. Extensive skeletal muscle cell mitochondriopathy distinguishes critical limb ischemia patients from claudicants. *JCI Insight*. 2018;3.

60. Park SY, Pekas EJ, Anderson CP, et al. Impaired microcirculatory function, mitochondrial respiration, and oxygen utilization in skeletal muscle of claudicating patients with peripheral artery disease. *Am J Physiol Heart Circ Physiol*. 2022;322:H867–H879.

61. Ryan TE, Kim K, Scali ST, et al. Interventional- and amputation-stage muscle proteomes in the chronically threatened ischemic limb. *Clin Transl Med*. 2022;12:e658.

62. Ferreira J, Carneiro A, Vila I, et al. Inflammation and loss of skeletal muscle mass in chronic limb threatening ischemia. *Ann Vasc Surg*. 2022.

63. Groennebaek T, Billeskov TB, Schytz CT, et al. Mitochondrial structure and function in the metabolic myopathy accompanying patients with critical limb ischemia. *Cells*. 2020;9:570.

64. Scott-Okafor HR, Silver KKC, Parker J, Almy-Albert T, Gardner AW. Lower extremity strength deficits in peripheral arterial occlusive disease patients with intermittent claudication. *Angiology*. 2001;52:7–14.

65. McDermott MM, Criqui MH, Greenland P, et al. Leg strength in peripheral arterial disease: associations with disease severity and lower-extremity performance. *J Vasc Surg*. 2004;39:523–530.

66. Morisaki K, Furuyama T, Matsubara Y, et al. Thigh sarcopenia and hypoalbuminemia predict impaired overall survival after infrainguinal revascularization in patients with critical limb ischemia. *Vascular*. 2020;28:542–547.

67. Matsubara Y, Matsumoto T, Aoyagi Y, et al. Sarcopenia is a prognostic factor for overall survival in patients with critical limb ischemia. *J Vasc Surg*. 2015;61:945–950.

68. McDermott MM, Liu K, Tian L, et al. Calf muscle characteristics, strength measures, and mortality in peripheral arterial disease: a longitudinal study. *J Am Coll Cardiol*. 2012;59:1159–1167.

69. White SH, McDermott MM, Sufit RL, et al. Walking performance is positively correlated to calf muscle fiber size in peripheral artery disease subjects, but fibers show aberrant mitophagy: an observational study. *J Transl Med*. 2016;14:284.

70. Barton-Davis ER, Shoturma DI, Sweeney HL. Contribution of satellite cells to IGF-I induced hypertrophy of skeletal muscle. *Acta Physiol Scand*. 1999;167:301–305.

71. Pelosi L, Giacinti C, Nardis C, et al. Local expression of IGF-1 accelerates muscle regeneration by rapidly modulating inflammatory cytokines and chemokines. *FASEB J*. 2007;21:1393–1402.

72. Stevens-Lapsley JE, Ye F, Liu M, et al. Impact of viral-mediated IGF-I gene transfer on skeletal muscle following cast immobilization. *Am J Physiol Endocrinol Metab*. 2010;299:e730–e740.

73. Zhang L, Wang XH, Wang H, Du J, Mitch WE. Satellite cell dysfunction and impaired IGF-1 signaling cause CKD-induced muscle atrophy. *J Am Soc Nephrol*. 2010;21:419–427.

74. Lin S, Zhang Q, Shao X, et al. IGF-1 promotes angiogenesis in endothelial cells/adipose-derived stem cells co-culture system with activation of PI3K/Akt signal pathway. *Cell Prolif*. 2017;50.

75. Sukhanov S, Higashi Y, Shai SY, et al. IGF-1 reduces inflammatory responses, suppresses

oxidative stress, and decreases atherosclerosis progression in ApoE-deficient mice. *Arterioscler Thromb Vasc Biol*. 2007;27:2684–2690.

76. Higashi Y, Sukhanov S, Anwar A, Shai SY, Delafontaine P. Aging, atherosclerosis, and IGF-1. *J Gerontol A Biol Sci Med Sci*. 2012;67:626–639.

77. Dobrowolny G, Giacinti C, Pelosi L, et al. Muscle expression of a local Igf-1 isoform protects motor neurons in an ALS mouse model. *J Cell Biol*. 2005;168:193–199.

78. Kahlert S, Nuedling S, van Eickels M, Vetter H, Meyer R, Grohe C. Estrogen receptor alpha rapidly activates the IGF-1 receptor pathway. *J Biol Chem*. 2000;275:18447–18453.

79. Venken K, Schuit F, van Lommel L, et al. Growth without growth hormone receptor: estradiol is a major growth hormone-independent regulator of hepatic IGF-I synthesis. *J Bone Miner Res*. 2005;20:2138–2149.

80. Leung KC, Johannsson G, Leong GM, Ho KKY. Estrogen regulation of growth hormone action. *Endocr Rev*. 2004;25:693–721.

81. McMillin SL, Minchew EC, Lowe DA, Spangenburg EE. Skeletal muscle wasting: the estrogen side of sexual dimorphism. *Am J Physiol-Cell Ph*. 2022;322:C24–C37.

82. Salyers ZR, Coleman M, Le D, Ryan TE. AAV-mediated expression of PFKFB3 in myofibers, but not endothelial cells, improves ischemic muscle function in mice with critical limb ischemia. *Am J Physiol Heart Circ Physiol*. 2022;323:H424–H436.

KEY WORDS **chronic limb threatening ischemia, gene therapy, regeneration, skeletal muscle**